Available online at www.sciencedirect.com
SCIENCE DIRECT®
Computer Vision and Image Understanding 103 (2006) 52–63
Computer Vision and Image Understanding
www.elsevier.com/locate/cviu

Natural color image enhancement and evaluation algorithm based on human visual system ☆

Kai-Qi Huang [a,*], Qiao Wang [b,1], Zhen-Yang Wu [b]

[a] National Laboratory of Pattern Recognition, Institute of Automation, Chinese Academy of Sciences, Beijing 100080, PR China
[b] Department of Radio Engineering, Southeast University, Nanjing 210096, PR China

Received 17 August 2004; accepted 25 February 2006
Available online 19 April 2006

Abstract

To a significant degree, multimedia applications derive their effectiveness from the use of color graphics, images, and videos. In these applications, human visual system (HVS) often gives the final evaluation of the processed results. In this paper, we first propose a novel color image enhancement method, which is named HVS Controlled Color Image Enhancement and Evaluation algorithm (HCCIEE algorithm). We then applied the HCCIEE to color image by considering natural image quality metrics. This HCCIEE algorithm is base on multiscale representation of pattern, luminance, and color processing in the HVS. Experiments illustrated that the HCCIEE algorithm can produce distinguished details without ringing or halo artifacts. (These two problems often occur in conventional multiscale enhancement techniques.) As a result, the experimental results appear as similar as possible to the viewers' perception of the actual scenes.

Keywords: Color image enhancement; Human visual system

1. Introduction

The goals of image enhancement can be differently stated depending on the particular application [1]. For natural color image, very often, human visual system (HVS) gives the final evaluation of the processed image. Two major problems need to be solved for natural image enhancement:

(1) more distinguished texture details,
(2) color of the processed image is perceptually better.

Numerous methods are available in the literature for texture details enhancement [2–6]. These methods can be classified into *denoising-based* enhancement and *contrast-based* enhancement. Deniosing-based approaches [4,6] give good performances upon gray-level images, while they normally cannot work well for color image enhancement. There are also many algorithms based on contrast-based enhancement, which has two major groups: (1) spatial uniform ones: the linear contrast stretch approach (also called windowing and leveling) and the histogram equalization approach are two of the most widely used spatial uniform contrast-based enhancement technique and (2) spatial non-uniform ones: adaptive histogram equalization (AHE), contrast-limited adaptive histogram equalization (CLAHE), and multiscale enhancement [2] are most representative spatial non-uniform contrast-based enhancement methods.

Techniques for enhancing color images have been similar to those for gray images. It seems to be an agreement that we can process each of the three monochrome images, say R, G, and B channels, separately and then combine the

☆ A preliminary and shortened version of this paper has been published in the Proceedings of IEEE Int'l Conf on Speech, Acoustics, and Signal Processing (ICASSP2004).

* Corresponding author. Fax: +86 10 6255 1993.
E-mail addresses: kqhuang@nlpr.ia.ac.cn (K.-Q. Huang), qiaowang@seu.edu.cn (Q. Wang), zhengyang@seu.edu.cn (Z.-Y. Wu).
[1] Fax: +86 25 8620 5037.

1077-3142/$ - see front matter
doi:10.1016/j.cviu.2006.02.007

three results. This implies that it is sufficient to enhance brightness only and in a sense, treat a color image like an achromatic one [4,11]. Another approach to color image enhancement is to transform the image data from RGB space to other color spaces such as LHS, HSI, YIQ, HSV, etc. In these color spaces several techniques have been developed such as the edge enhancement techniques [8,9], simple global saturation stretching [12,13], complex diffusion processes [4,14,15], hue dependent saturation histogram equalization [16], and intensity edge enhancement based on saturation [17,18]. Naik puts forward a hue-preserving image enhancement method to solve the gamut problem by space transforming and processing in these spaces [7]. While these methods just focus on detail enhancement and do not consider perception color enhancement. Two worth mentioned "psychophysically derived" color enhancement methods are Faugeras' homomorphic model [10] and Jobsen's Retinex model [19,20], which both consider the human eyes model to enhance color image. In [10] not only details and dynamic range are enhanced but also color constancy is achieved by simple homomorphic model, which causes color enhancement effectiveness is not good enough. Jobsen considers more complex human eyes model—Retinex (retina and cortex) theory by Land and gets a better color enhancement method, which achieves sharpening, color constancy, and dynamic range compression.

For color image, another basic limitation of developing enhancement algorithms is the lack of a quantitative measure of image quality. However, color image quality metrics remain unclear and we should consider the properties of the HVS for color image enhancement.

We have been investigating the image processing techniques based on HVS properties [3,21,22]. In this paper, based on HVS models, a novel color image enhancement algorithm, Human visual system Controlled Color Image Enhancement and Evaluation (HCCIEE) algorithm, is presented. The method for color image enhancement consists of multiscale representation of pattern, luminance, and color processing in the HVS. First, wavelet-based enhancement method with contrast sensitive functions (CSFs) are used to enhance R, G, and B components, respectively. Second, the color of image is adjusted according to natural image quality metrics [23,24] by suitable manipulation of the psychophysically derived color naturalness index (CNI) and color colorfulness index (CCI). Our technique proves to be useful to produce the nearly best looking image[2] because human visual characteristics such as brightness and contrast, which is concerned with details [3], and perception color are considered to enhance the texture details and color. Finally, we also give the evaluation of the processed image's quality in terms of naturalness and colorfulness.

[2] It should be mentioned that the processed image by our algorithm will have no reference portion as was the case in Pappas and Pitas' use of a small restored section of a larger degraded painting [25].

This paper is organized as follows: Section 2 presents the HCCIEE algorithm for color enhancement. Section 3 reports some experimental results and provides corresponding analyses. Thereafter, Section 4 concludes.

2. The HCCIEE algorithm based on HVS Model

2.1. The HCCIEE algorithm

The flow of HCCIEE algorithm is depicted in Fig. 1. Our algorithm consists of two stages: (1) enhancing the texture details and avoiding artifacts such as ringing or halo. In this level, the multiscale characteristics and CSFs will be considered; (2) rendering the color of image according to natural image quality metrics. The color will be decided by CNI and CCI, which are psychophysically derived and achieved by some statistics values from natural images. We show that the combination of these two-level operations is effective in enhancing the quality of color image.

2.1.1. Wavelet-based image enhancement method with contrast sensitivity functions

Classical methods of contrast enhancement, e.g., histogram specification, suffer from the drawbacks of treating all areas of the image uniformly. Some improvements have been obtained by using adaptive methods [1]. However, such methods do not measure the contrast. In addition, disregard spatial features which may differ considerably from one region to another. Improved performances have been obtained by introducing locally adaptive measures of

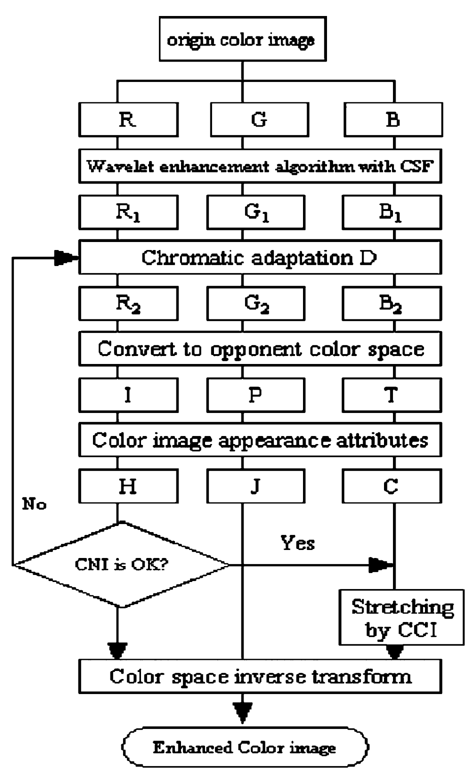

Fig. 1. The flow of HCIEE algorithm.

contrast. For instance, in [26] edge information is incorporated in the computation of local contrast. One critical aspect of locally adaptive methods is that local contrast has to be evaluated for each pixel (x, y) of the image domain, inside its corresponding windows centered at it. Unfortunately, there is not a general rule to produce the optimal size of these varying windows. This problem has led to multiscale methods based on wavelet transforms [27]. These techniques modify the wavelet coefficients of the image decomposition at different scales and obtain a contrast enhanced image. Wavelet-based methods can be more effective than locally adaptive ones, provided that the number of scales is appropriately chosen and the coefficient transformation is suitably designed [7]. Otherwise, reconstruction may become unstable with respect to the origin image, and ringing artifacts (over-enhancement) or halo artifacts may occur [28,29]. In our prior work [3], we have reported an algorithm to gray image enhancement that exploits the multiscale wavelet and statistical characters of visual representation. Processing includes the global dynamic range (brightness) correction and local contrast adjustment, whose parameters are picked automatically by the information contained in the image itself. The algorithm achieves some effectiveness in gray image enhancement. In this section, we present a novel approach that combines threshold model of vision, considering contrast sensitivity functions (CFSs) with wavelet transformation to enhance the brightness and details without inducing artifacts.

2.1.1.1. General wavelet-based enhancement algorithm. The product of the wavelet transform is a hierarchy of resolution information at many different scales and orientations [30]. At each level, the wavelet transform can be re-applied to the low-resolution sub-band to further decompose the image. The general framework of a filter bank implementation of an over-completely multiscale enhancement is schematically illustrated in Fig. 2. $A_{j+1}f$ is the low resolution residual. The $D^1_{j+1}f, D^2_{j+1}f, D^3_{j+1}f, j = 1, 2, \ldots, J-1$ are called the details, where j is the level, with J being the largest scale. Redundancy is exploited by first modifying transform coefficients in the transform domain and then reconstruction. For image f, it may be characterized as

$$A_jf = A_{j+1}f + D^1_{j+1}f + D^2_{j+1}f + D^3_{j+1}f \tag{1}$$

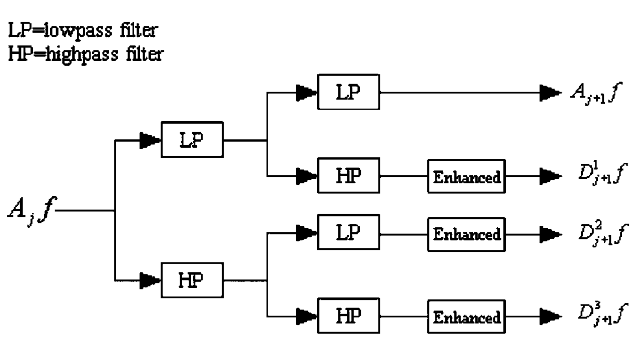

Fig. 2. Multiscale expansion with enhancement for 2 level analysis.

the enhanced image is

$$\tilde{A}_jf = \tilde{A}_{j+1}f + \left[F^1_{j+1}\left(D^1_{j+1}f\right) + F^2_{j+1}\left(D^2_{j+1}f\right) + F^3_{j+1}\left(D^3_{j+1}f\right)\right], \tag{2}$$

where $F^i_{j+1}(i = 1, 2, 3)$ is called oriented enhancement gain function or mapping function, which can be implemented independently of a particular set of filters and easily incorporated into a filter bank to provide the benefits of multiscale enhancement. For simplicity, we let three oriented mapping functions are same. The algorithms developed by Lain and others [31] have typically included the use of non-mapping functions to process the wavelet coefficients. A variety of such functions have been reported in the literature [19,27,32,33]. But the ringing artifacts or halo artifacts still often occur for these multiscale enhancement algorithms because of gain functions F^i_{j+1} [28,29][3]. The artifacts can be significantly reduced if human visual properties are included in the design of mapping functions. Next we shall present a wavelet enhancement algorithm based on the threshold model of human vision.

2.1.1.2. Threshold model of vision—contrast sensitivity functions in spatial and frequency domain. The HVS is a non-linear system which has a very large dynamic range and behaves as a band-pass spatial filter [34]. The spatial filtering property is characterized by CSF which is the reciprocal of the threshold contrast. The threshold contrast is a function of both spatial frequency and background luminance. The smallest luminance difference that human observer can detect when an object of a certain size is displayed at a certain background luminance level is defined as the Just-Noticeable-Difference (JND). The threshold model of vision describes the JND in luminance that the eyes are able to perceive in a given situation.

To give some intuition about contrast sensitivity, some rules are as follows:

- the contrast perception keeps constant at very high luminance and/or low spatial frequency, this independence of luminance is called Weber's Law [35];
- the contrast perception and the color saturation increase with luminance (Hunt effect [37] and Stevens effect [36]). This is generally true, except at very high luminance or very low frequency. This rule is sometimes referred to sub-Weber behavior [38];
- at low spatial frequency, the contrast sensitivity increases linearly with frequency [30].

The effects of contrast sensitivity have been measured in threshold experiments. Fig. 3A shows the result of a threshold experiment that measured the changes in visibility occurring with changes in the level of illumination. The

[3] The à trous wavelet transform algorithm instead of FWT was often used to avoid the coherent ringing artifacts of it [46]. This paper we mainly do with the halo artifacts.

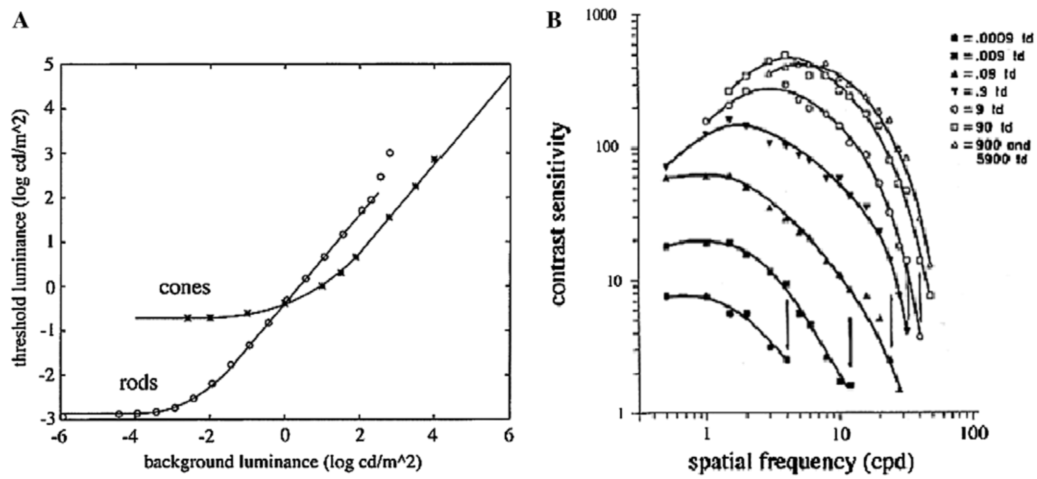

Fig. 3. Threshold models of vision: (A) threshold *vs* intensity (TVI) function for the rod and cone systems. The curves plot the smallest threshold increment ΔL necessary to see a spot against a uniform background with luminance L. (B) Contrast sensitivity functions for sinusoidal gratings illuminated at different mean luminance levels. Levels are specified in Troland (Td) units of retinal luminance (Trolands = luminance in cd/m^2 $\times$ pupil area) [35,37].

curves plot the smallest luminance increment ΔL that can be detected at a particular background luminance L and are known as threshold-vs.-intensity (TVI) functions. The two curves show the TVI functions for the rod and cones systems. The linear relationship $\Delta L = KL$ is known as Weber's law and indicates that the visual system has constant contrast sensitivity since the Weber contrast $\Delta L/L$ is constant over this range. The HVS's response to complex objects can be modeled by the CSFs. Here the contrast sensitivity is defined as a (1/threshold contrast) using the Michelson definition of contrast: $(L_{\max} - L_{\min})/(L_{\max} + L_{\min})$, where $L_{\max}$ and $L_{\min}$ are the luminance at the peaks and troughs of the sinusoidal gratings [39]. Fig. 3B shows the contrast sensitivity varies with spatial frequency and the changes of luminance adaptation. It has been measured for an achromatic signal, at different frequencies and luminance levels. The contrast sensitivity function increases with increasing luminance level, thus shows a sub-Weber behavior, until it reaches a particular value and stays constant.

The CSFs are sometimes called visual acuity [40], which can be combined with conventional enhancement algorithm to control degree of the details enhancing.

2.1.1.3. Details enhancement based on wavelet and threshold model of human vision. We can choose the cone's TVI-like functions, which represent threshold of the cone system and the growth in response required to allow perceived contrast to increase with luminance level (sub-Weber's law behavior), as the gain functions. The cones are called daylight vision, which adapt much more rapidly to change of light levels and color. Rods are responsible for dark adaptation, or scotopic vision, which are not used in most image processing. The gain function is given for the cones in the following equation as shown in Fig. 4 [21,38]

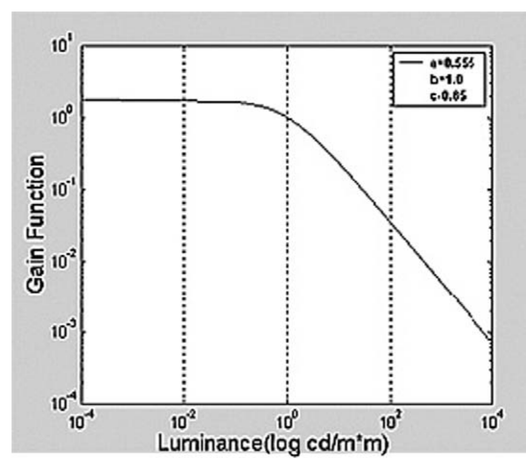

Fig. 4. Luminance gain function (1/TVI), the parameters $a = 0.555$, $b = 1.0$, and $c = 0.05$ [21,38].

$$G(I) = \frac{1}{a(I+b)^c}. \tag{3}$$

In the above equation, I represents the cone signal that is used to set the level of adaptation and $G(I)$ is the gain function. Eq. (3) is derived to match available psychophysical TVI and brightness matching data. The constants a, b, and c are chosen as Fig. 4. In the wavelet inverse transform, the details enhancement function (mapping function) can be decided as the following equation

$$\tilde{F}_j(D_j f) = G\left(A_{j+1}f + \tilde{F}_{j+1}\left(\sum_{i=1}^{3} D^i_{j+1}f\right)\right). \tag{4}$$

The initial function is as followed:

$$\tilde{F}_J = G(A_J f), \tag{5}$$

where i is the wavelet orientation, the gain function will be same in different orientation so as to reduce computation cost, $A_J f$ is the low-pass residual which contains much of the luminance distribution. The enhanced images are analogous to the contrast images that Peli obtained [41]. By this way, we define local band-limited contrast in images that assigns a contrast value to every point in the image as a function of the spatial frequency band. For each frequency band, the contrast is defined as the ratio of the sub-band filtered image at the frequency to the low-pass image filtered to an octave below the same frequency (local luminance mean), the magnitude of these images is a function of luminance level as specified by the gain functions. This is necessary to allow prediction of luminance-dependent appearance effects. With the wavelet reconstruction, we can obtain CSFs and details can be enhanced with the change of luminance adaptation (as Fig. 3B) in some degree so that the details enhancement in every sub-band is not randomly but decided by human perception.

2.1.2. Color rendition according to natural image quality metrics

Running the first step of HCCIEE algorithm will return an image which looks more distinguished but may be unnatural or unvivid. A suitable color re-rendition operation is thus necessary. Before color rendition, we will introduce natural color image quality metrics firstly.

2.1.2.1. Color image quality metrics. There has been significant research on image quality metrics [21,44,45], which often aim at the creation and optimization of encoding/compression/decoding algorithms such as MEPG2 and MPEG4. In our enhancement algorithm, we want to produce the best looking image rather than achieve luminance and color fidelity. Two main factors have to be considered when we design color image quality metrics: naturalness and colorfulness. Naturalness is the degree of correspondence between human perception and reality world, which is described by CNI here; Colorfulness presents the color vividness degree, which is described by CCI here. Yendrikhovskij introduces a model for optimal color image reproduction of natural images which are based on the assumption that color quality of natural images is constrained by perceived naturalness and colorfulness of these images [23]. Recently, Hasler [24] gives a more accurate metrics for colorfulness, which is used in our algorithm.

In the paper, the CNI can be computed as follows:

[Step1:] Transforming color image in RGB space to other color space such as CIELUV color space.
[Step2:] Computing the luminance (L), hue (H), and saturation (S), respectively.
[Step3:] Thresholding L and S components: L values between 20 and 80 are kept, S values over 0.1 are kept.
[Step4:] Defining three kinds of pixels according to hue value: 25–70 is called "skin" pixels, 95–135 is called "grass" pixels, and 185–260 is called "sky" pixels.
[Step5:] Calculating averaged saturation values for "skin" $S_{\text{average\_skin}}$, "grass" $S_{\text{average\_grass}}$, and "sky" $S_{\text{average\_sky}}$ pixels and numbers of "skin" pixels n_{skin}, "grass" pixels n_{grass}, and "sky" pixels n_{sky}.
[Step6:] Calculating local CNI values for "skin," "grass," and "sky" pixels:

$$N_{\text{skin}} = \exp(-0.5 * ((S_{\text{average\_skin}} - 0.76)/0.52)^2),^4 \quad (6)$$

$$N_{\text{grass}} = \exp(-0.5 * ((S_{\text{average\_grass}} - 0.81)/0.53)^2), \quad (7)$$

$$N_{\text{sky}} = \exp(-0.5 * ((S_{\text{average\_sky}} - 0.43)/0.22)^2). \quad (8)$$

[Step7:] Calculating the global CNI values:

$$N_{\text{image}} = (n_{\text{skin}} * N_{\text{skin}} + n_{\text{grass}} * N_{\text{grass}} + n_{\text{sky}} * N_{\text{sky}})/ \times (n_{\text{skin}} + n_{\text{grass}} + n_{\text{sky}}) \quad (9)$$

N_{image} varies from 0 (the most unnatural image) to 1 (the most natural image).

The colorfulness index C_k is defined as Eq. (10)

$$C_k = S_k + \sigma_k, \quad (10)$$

where S_k is the average saturation of image k, σ_k is standard deviation, noting that C_k varies form 0 (achromatic image) to $C_{\max}$ (most colorful image).

The naturalness index and colorfulness index are derived by fitting naturalness and colorfulness judgments using a least squares fitting procedure. As can be seen in Fig. 5, the correlation between the obtained naturalness index (CNI) and naturalness scores reported is $r = 0.87$ and explains the major variability in their experimental data. The colorfulness correlation is 0.91. Recently, Hasler [24] gives a very nice and efficient way of computing the colorfulness. He assumes that the image is coded in the sRGB color space and gives a new colorfulness metric:

$$C_k = \sigma_{rgyb} + 0.3 \cdot \mu_{rgyb}, \quad (11)$$

$$\sigma_{rgyb} = \sqrt{\sigma_{rg}^2 + \sigma_{yb}^2}, \quad (12)$$

$$\mu_{rgyb} = \sqrt{\mu_{rg}^2 + \mu_{yb}^2}, \quad (13)$$

where rg and yb are the components in sRGB color space. The correlation of C_k with the experimental data is equal to 95.3%.

According to [23], the range of CNI is from 0 to 1, the closer to 1 CNI is, the more natural color image is. The best range for CCI is 16–20, which shows that the color of image in this range will be suitable for human.

2.1.2.2. Color rendition. In the above section, color naturalness index (CNI) and color colorful index (CCI) are defined to evaluate natural color image metrics and we also get the

[4] Values 0.76, 0.52, 0.81, 0.53, 0.43, and 0.22 are determined experimentally [23].

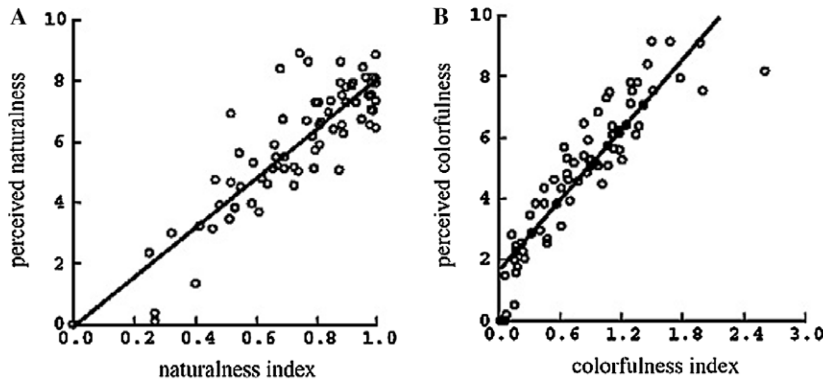

Fig. 5. (A) Naturalness judgment *vs* the naturalness index. (B) Colorfulness judgments *vs* the colorfulness index [23].

optimal values for these two indices, then we carried out color rendering by simple chromatic adaptation model among enhanced R, G, and B components. The chromatic adaptation model [42], given in Eqs. (14)–(16), is a linear von Kries normalization of RGB image signals:

$$R_2 = \left[\left(L_1 \frac{D}{R_1}\right) + (1-D)\right] R_1, \tag{14}$$

$$G_2 = \left[\left(L_1 \frac{D}{G_1}\right) + (1-D)\right] G_1, \tag{15}$$

$$B_2 = \left[\left(L_1 \frac{D}{B_1}\right) + (1-D)\right] B_1, \tag{16}$$

where L_1 is luminance which can be computed as a weighed sum of pixels in the $R_1G_1B_1$ components of the color image. The von Kries normalization is modulated with a degree-of-adaptation factor D, which can vary from 0 for no adaptation to 1 for complete chromatic adaptation. The D factor can be established manually or given in GW (Gray World assumption) method or illuminant estimation by the maximum of each channel [42]. We choose D according to CNI, one of color metrics. The next stage of HCCIEE algorithm is to enhance colorfulness. The image is converted from *RGB* signals (roughly analogous to cone signals in the HVS) to opponent-color signals (light–dark, red–green, and yellow–blue; analogous to higher-level encoding in the HVS) that are necessary for constructing a uniform perceptual color space. In choosing this transformation, simplicity, accuracy, and applicability to image processing are the main considerations. The color space chosen is the IPT space published by Ebner and Fairchild [43], which is derived specifically for image processing application to have a hue-angle component with good prediction of constant perceived hue. Once the IPT coordinates are computed for the image, a simple coordinate transformation is applied to obtain image-wise predictors of lightness (J), chroma (C), and hue angle (H) as formula: (17)–(19)

$$J = I, \tag{17}$$

$$C = \sqrt{P^2 + T^2}, \tag{18}$$

$$H = \tan^{-1}\left(\frac{P}{T}\right). \tag{19}$$

Here, we only simply stretch the chroma to enhance the image colorfulness. β can be chosen by another color metrics CCI

$$C_1 = C^{\beta}. \tag{20}$$

3. Experimental results

To verify the effectiveness of the proposed method, experiments are performed with a set of 24-bit color images. In our experiments, the à trous wavelet transform algorithm instead of FWT is used to avoid the coherent ringing artifacts [46], we also use the wavelet in [46] for convenience.

HCCIEE algorithm is tested in two ways:

First, we compare HCCIEE algorithm with other color image enhancement methods. There are many excellent methods in the field of signal/image processing and computer graph algorithm with the same goal such as work by Pattanaik [38]. Here, we pay more attention to the prior field. We have given an introduction about color image enhancement methods in Section 1, most of which concern on enhancing the details of image texture while preserving the color and most TRC or TRO techniques also concern on image brightness including Peli's method, multiscale Retinex color restoration (MSRCR) algorithm [19] is outstanding compared with other state-of-the art color image enhancement technique as it is used to achieve sharpening, color constancy, and dynamic range compression, so we compared with it. The results are shown in Fig. 6. Fig. 6A is the origin image "Paris in night." The image quality is not good in local lightness. Especially parterre is in poor visual condition. Fig. 6B is the enhanced result of the histogram equalization (HE) only in luminance components, from which we can see that there is something (such as parterre) in dark part of image, but it is over-enhanced for this image. Compared with other gray image enhancement methods in luminance component without considering color information, our HCCIEE algorithm is psychophysically derived and "global" in its attempt to

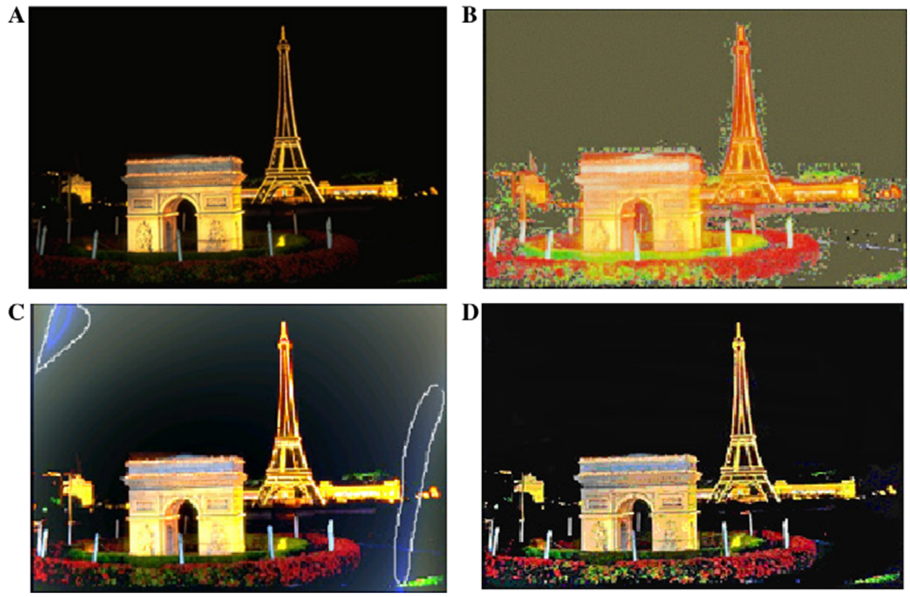

Fig. 6. (A) is the origin image "Paris in night," (B) the enhanced result by the HE only in luminance components. (C) The enhanced result by multiscale Retinex color restoration (MSRCR) algorithm, halo artifacts marked with white lines. Gain factor is [250,80,15]. (D) The result of HCCIEE algorithm. (For interpretation of the references to color in this figure legend, the reader is referred to the web version of this paper.)

generate an overall pleasing image with respect to color. Fig. 6C is the enhanced result of MSRCR algorithm. The MSRCR algorithm is an excellent color image enhancement algorithm recently, the parterre and other objects can be seen clearly, the colorfulness is also better than that of Fig. 6A because it considers color constancy. It is a multiscale enhancement algorithm with the gain function used being constant, 250, 80, and 15, respectively, which causes halo artifacts in shadow part of image marked with white line (severe blue coloration at the TL and BR corners of the image) in Fig. 6C. Fig. 6D is the result of our HCCIEE algorithm. We can see that the multiscale characteristics make the parterre and other objects the same clearer as Fig. 6C, the color effect is also close to Fig. 6C, but the halo artifacts in Fig. 6C are reduced because the gain functions are chosen according to HVS, the details in Fig. 6D are better than those of Fig. 6D too. We also give some comparison results to test the first stage of our HCCIEE algorithm with four different enhancement algorithms. Test image is a kind of high range dynamic gray image (HRD) whose ratio between the brightest part and the darkest part is very large [48]. The first method applied is the HE. The second algorithm is CLAHE. The third method is the result by previous wavelet method [11]. We do not compare our results with AHE and JGACE algorithms, because the results of CLAHE are better than the former and similar to JGACE in most cases if background noise is low. The fourth technique employed for comparison is the first stage of our HCCIEE algorithm. From the results shown in Fig. 7, it is clear that HE causes a saturation for the high illumination areas (park entrance) and over-enhanced this area while other area enhanced less, CLAHE are better than HE and enhanced local areas by blocks. But the result shows some artifact block effect and the enhanced image looks unnatural, the previous wavelet enhancement method has little effect on this image because of not considering luminance enhancement while our algorithm achieves the best effectiveness both in luminance and details.

Second, after enhancing the luminance and texture details, we will adjust the image color in the second stage. Two main factors have to be considered in this stage: naturalness and colorfulness. Naturalness is the degree of correspondence between human perception and reality world, which is described by color naturalness index (CNI) here; Colorfulness presents the color vividness degree, which is described by color colorfulness index (CCI). Naturalness is more important than colorfulness for color image, so we first adjust the naturalness by chromatic adaptation model [42], where the parameter D can be decided by the psychophysically derived metrics CNI. CNI is one of the metrics from a large amount of color image by experts and is normalized from 0 to 1, the closer to 1, the more natural is. The colorfulness will be adjusted in succession. The original color image should be achieved better both in naturalness and colorfulness. We test the second stage of HCCIEE algorithm by human perceptual way with the evaluation metrics: naturalness and colorfulness. The results are shown in Fig. 8. Fig. 8A is the origin image "hut and sheep" from [47], which is bad for details and green-color-shifting. Fig. 8B is the result after the step of details enhancement and naturalness processing. The details are more clarity and the color shifting is corrected to natural scene, but the colorfulness is not enough and the image is not vivid. Fig. 8C is the result of colorfulness processing continued. The image is better than Fig. 8B in colorfulness. Fig. 9A is another color- shifting image "fruit under sun," which is often used for color constancy [42]. Fig. 9B is the

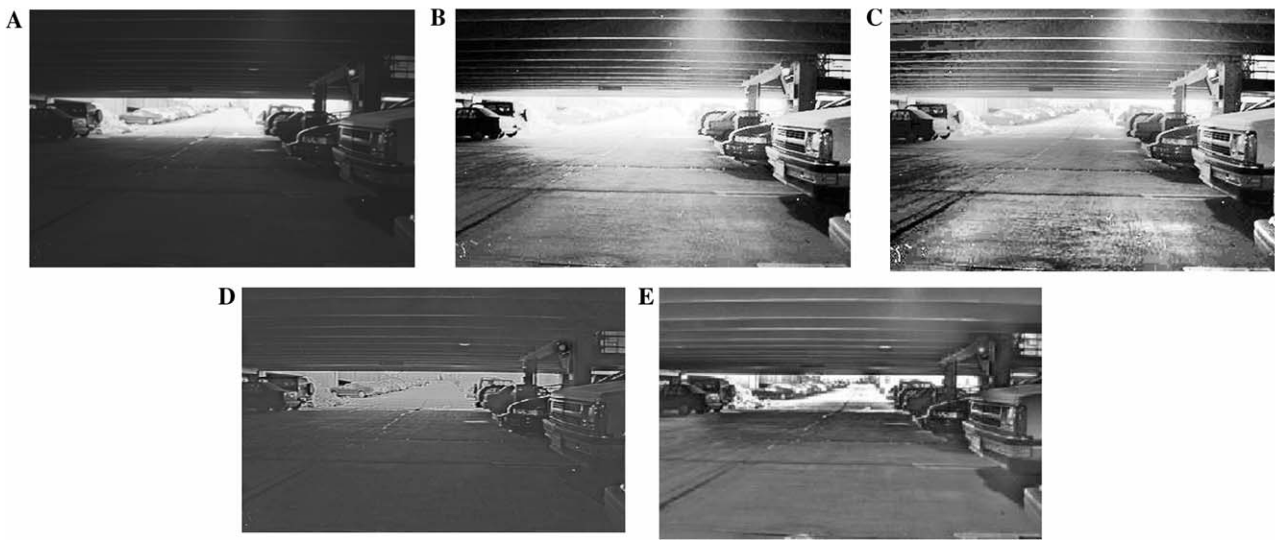

Fig. 7. Example result of several image enhancement algorithms: (A) original image, (B) histogram equalization result, (C) CLAHE result, (D) wavelet method [11], and (E) result of the first stage processing of our HCCIEE algorithm.

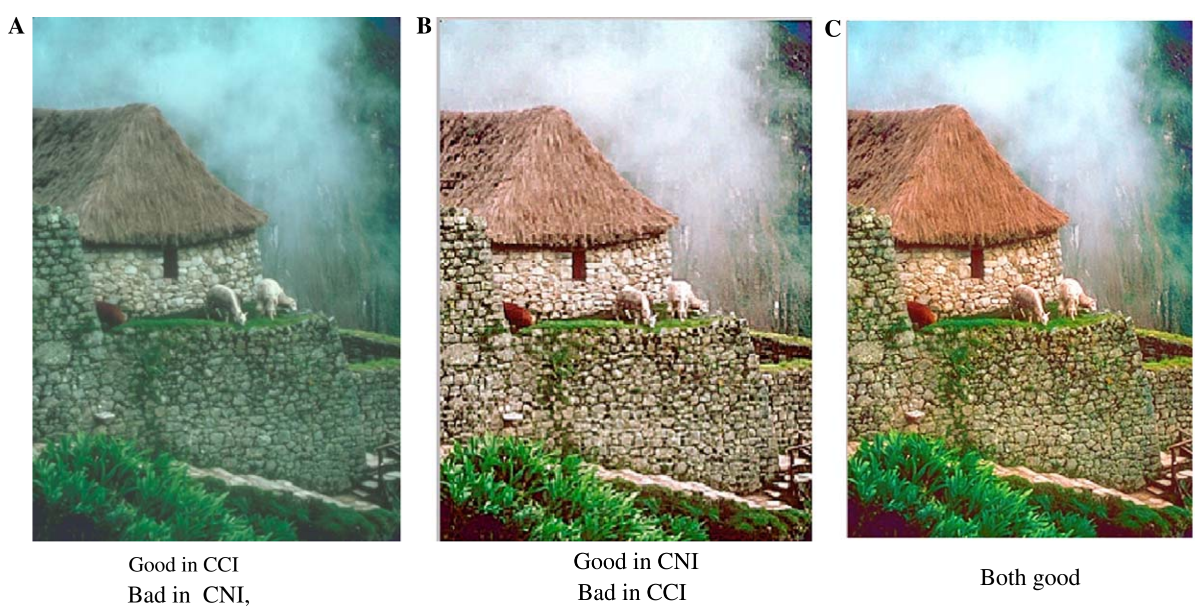

Fig. 8. (A) Origin image "hut and sheep," (B) naturalness processed image, and (C) HCCIEE algorithm. (For interpretation of the references to color in this figure legend, the reader is referred to the web version of this paper.)

result of naturalness processing, which is improved greatly.

This can also be testified by metrics in Table 1. For Fig. 8, we can see that CNI is 0.6712, far away from 1, but the CCI is 16.6033, between 16 and 20, which shows that (A) is bad in color naturalness but good in color colorfulness (15–20 is quite colorfulness by experiments [21]). Fig. 8B, CNI is 0.9534 and CCI is 9.3497, which shows the naturalness is improved but the colorfulness is not enough good, after the HCCIEE processing, CNI and CCI of Fig. 9C are 0.9578 and 15.9675, which shows both naturalness and colorfulness are optimal by experimental results. For Fig. 9A, the image is also bad in naturalness but good in colorfulness (CNI and CCI are 0.5126 and 16.7568), after the naturalness processing, Fig. 9B achieves good in naturalness (CNI is 0.9726) and colorfulness (19.5132), so no colorfulness adjusting needed. We also give other real scene examples as Figs. 10–12. (A) is the original real scene color image captured by canon digital camera in auto-model sets and (B) is the image enhanced by our algorithm. We can see that the quality of photos captured by camera can be improved better in details, lightness and color by our HCCIEE algorithm. To validate the effectiveness, we test our algorithm on the large sample natural color images, which consisted of image from internet database and real scene captured by canon A60. Fig. 13 is the statistical

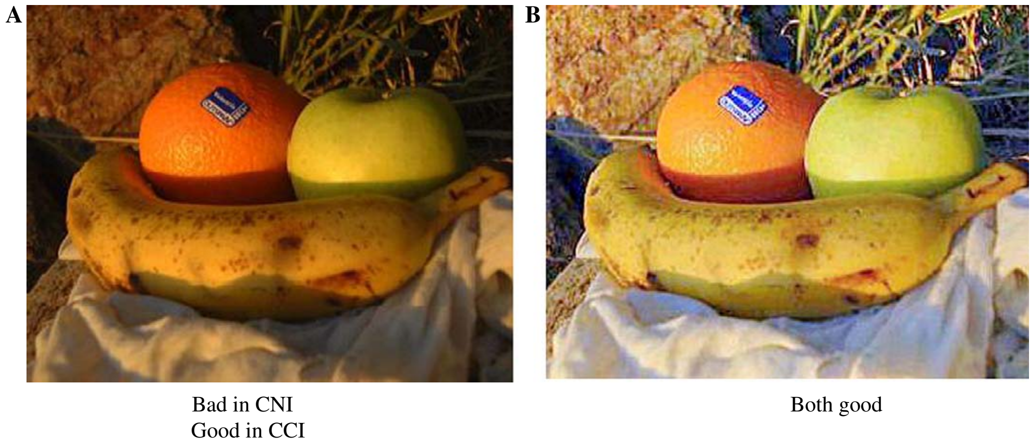

Fig. 9. (A) Origin image, (B) naturalness processed image.

Table 1
Measure naturalness and colorfulness

Images\metrics	Fig. 8. "hut and sheep" [47]			Fig. 9. " fruit under sun" [42]	
	Origin (A)	Naturalness processed (B)	HCCIEE algorithm (C)	Origin (A)	Naturalness processed (B)
Color naturalness index (CNI: 1 is best)	0.6712 (bad)	0.9534 (good)	0.9578 (good)	0.5126 (bad)	0.9726 (good)
Color colorfulness index (CCI: 16–20 is good)	16.6033 (good)	9.3497 (bad)	15.9675 (good)	16.7568 (good)	19.5132 (good)

Fig. 10. (A) Original image captured by canon digital camera in auto-model sets CCI = 0.7238 and CCI = 15.1172. (B) HCCIEE algorithm enhanced color image CCI = 0.9418 and CCI = 19.2317.

results of CCI and CNI of 1000 test images including all testing result in the paper. Circle "○" stands for original color image and circle "•" stands for enhanced color image. It is clear that the CNI/CCI of original image is evenly distributed and CNI/CCI of enhanced image is strongly clustered. The horizontal axes are the CNI/CCI value and vertical axes are the image number index. The nearer to 1 CNI is, the better the images are, the CCI is clustered between 16 and 20, which is consistent with our analyzing.

4. Conclusion

We present a novel algorithm for color image enhancement, which consists of wavelet-based detail enhancement operation and the color rendition. We give

Fig. 11. (A) Original color image captured by canon digital camera in auto-model sets CCI = 0.7781 and CCI = 21.2713. (B) HCCIEE algorithm enhanced color image CCI = 0.9732 and CCI = 19.6171.

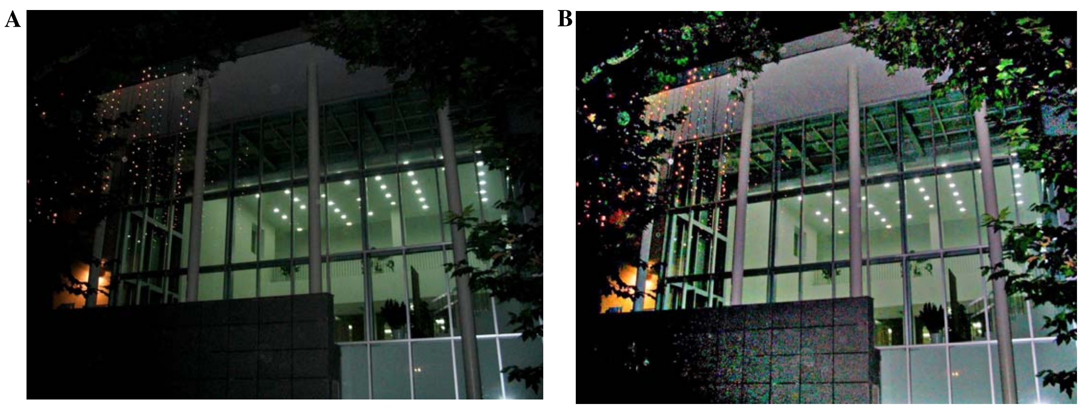

Fig. 12. (A) Original color image captured by canon digital camera in auto-model sets CCI = 0.4813 and CCI = 13.7312. (B) HCCIEE algorithm enhanced color image CCI = 0.9398 and CCI = 19.4715.

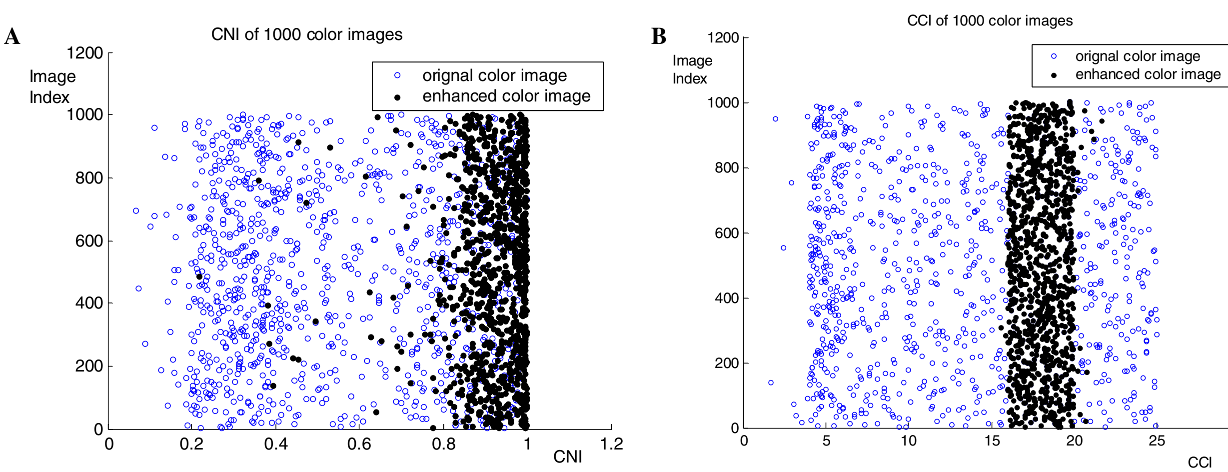

Fig. 13. Statistical results of (A) CNI and (B) CCI of 1000 test images including all testing figures in the paper The horizontal axes are the CNI/CCI value and vertical axes are the image number index.

a few examples that show the effectiveness of this technique in sharpening the texture details and rendering colors with an image thereby improving its appearance. We have also shown that the algorithm includes a subjective level in evaluating the result image, which proves to be more robust in achieving visually enhanced output images. This functionality may be useful in application concerned with image and video such as visual surveillance and retrieval. For visual surveillance, especially abnormal behavior analysis under low lightness condition as night, the first stage of our algorithm can be used to obtain better quality of image or video by luminance and details preprocessing. Our algorithm is also very useful for image or photo retrieval, we can obtain perceptual optimal results for old painting or photos after adjusting details and color. In the future, there are also many works need to be done in color quality metrics and the HVS parameters provided from psychophysical data, how to establish relation between psychophysically derived CCI and CNI and mathematical representation will be also considered in the future. Another important factor is trade-off between algorithm speed and effectiveness. We pay more attention to visual effect. In the future, we will mainly focus on how to make the algorithm faster for video-based applications.

Acknowledgments

This work is supported by National Key Basic Research Projects of China 973 Grant (2002 CB312102). The authors would like to thank Dr. S.Yendrikhovskij (Kodak Corporation) for the discussion of Perceptually Optimal Color Reproduction and Prof. Daniel, J. Jobsen (NASA) for the discussion of MSRCR algorithm. The authors like to thank the four anonymous reviewers and the editor for their valuable comments.

References

[1] G. Sharma, M.J. Vrhel, H.j. Trussell, Color imaging for multimedia, Proc. IEEE 86 (6) (1998) 1088–1108.
[2] Rafael C. Gonzalez, Richard E. Woods, Digital Image Processing, Addison-Wesley, Reading, MA, 2002.
[3] Kaiqi Huang, Zhen-yang Wu, Qiao Wang, Image enhancement based on the statistics of visual representation, Image Vision Comput. 23 (2005) 51–57.
[4] G. Gilboa, N. Sochen, Y.Y. Zeevi, Image enhancement and denoising by complex diffusion processes, IEEE Trans. PAMI 26 (8) (2004) 1020–1036.
[5] T. Jinshan, E. Peli, S. Acton, Image enhancement using a contrast measure in the compressed domain, Signal Process. Lett., IEEE 10 (10) (2003) 289–292.
[6] Kaiqi Huang, Zhenyang Wu, George S.K. Fung, Francis H.Y. Chan, "Color image denoising with wavelet thresholding based on Human Visual System Model", Signal Process.: Image Commun. 20 (2) (2005) 115–127.
[7] S.K. Naik, C.A. Murthy, Hue-preserving color image enhancement without gamut problem, IEEE Trans. Image Process. 12 (12) (2003) 1591–1598.
[8] A. Polesel, G. Ramponi, V.J. Mathews, Image enhancement via adaptive unsharp masking, IEEE Trans. Image Process. 9 (3) (2000) 505–510.
[9] W. Yu-Ping, Qiang Wu, K.R. Castleman, Zixiang Xiong, Chromosome image enhancement using multiscale differential operators, IEEE Trans. Med. Imaging 22 (5) (2003) 685–693.
[10] O. Faugeras, Digital color image processing within the framework of a Human Visual Model, IEEE Trans. Acoust. Speech Signal Process. 27 (4) (1979) 380–393.
[11] A. Toet, Multi-scale color image enhancement, Pattern Recogn. Lett. 13 (1992) 167–174.
[12] T. Kokkeong, J.P. Oakley, Enhancement of color images in poor visibility conditions, Proc. IEEE Intl. Conf. Image Process. 2 (2000) 788–791.
[13] L. Lucchese, S.K. Mitra, A new algorithm based on saturation and desaturation in the *xy* chromaticity diagram for enhancement and rendition of color images, Proc. IEEE Intl. Conf. Image Process. (2001) 7–10.
[14] B.T. ang, G. Sapiro, V. Caselles, Color image enhancement via chromaticity diffusion, IEEE Trans. Image Process. 10 (5) (2001) 701–707.
[15] L. Lucchese, S.K. Mitra, A new class of nonlinear filters for color image processing: theory and applications, IEEE Trans. Image Process. 13 (4) (2004) 534–548.
[16] V. Buzuloiu, M. Ciuc, R.M. Ranayya, C. Vertan, Adaptive-neighborhood histogram equalization of color images, J. Electron. Imaging 10 (2) (2001) 445–459.
[17] R.N. Strickland, C.S. Kim, W.F. McDonnell, Digital color image enhancement based on the saturation component, Opt. Eng. 6 (7) (1987) 609–616.
[18] B.A. Tomas, R.N. Strickland, Color image enhancement using spatially adaptive saturation feedback, Proc. IEEE Intl. Conf. Image Process. 3 (1997) 30–33.
[19] Daniel J. Jobsen, Ziaur Rahman, Glenn A. Woodell, Properties and performance of a center/surround Retinex, IEEE Trans. Image Process. 6 (3) (1997) 81–96.
[20] G. Orsini, G. Ramponi, P. Carrai, R. Di Federico, A modified Retinex for image contrast enhancement and dynamics control, ICIP2003 3 (2003) 14–17, 393-396..
[21] Kaiqi Huang, Zhenyang Wu, Color image denoising with wavelet thresholding based on Human Visual System model, Proc. Visual Communication and Image Process. Conference (VCIP2003), Lugano, Switzerland, July 8–11, 5150 (2003) 1667–1676.
[22] Kai-Qi huang, Qiao Wang, Zhen-yang Wu, Color image enhancement and evaluation algorithm based on human visual system Proc. of the International Conference of Speech, Acoust., and Signal Process. (ICASSP04), Montreal, Canada, III (2004) 721–724.
[23] S. Yendrikhovskij, F. Blommaert, H. de Ridder, Perceptually optimal color reproduction, Proc. SPIE: Hum. Vision Electron. Imag. III 3299 (1998) 274–281.
[24] S. Hasler, S. Süsstrunk, Measuring colorfulness in real images, Proc. SPIE Electron. Imag.: Hum. Vision Electron. Imag. VIII, SPIE 5007 (2003) 87–95.
[25] M. Pappas, I. Pitas, Digital color restoration of old paintings, IEEE Trans. Image Process. 9 (2) (2000) 291–294.
[26] A. Beghdadi, A. Le Negrate, Contrast enhancement techniques based on local detection of edge, Comp. Vis., Graph. Image Proc. 46 (1989) 162–174.
[27] J. Lu, Dennis M. Healy Jr., John B. Weaver, Contrast enhancement of medical images using multi-scale edge representations, Opt. Eng. 33 (7) (1994) 2151–2161.
[28] J.M. Dicarlo, B.A. Wandell, Rendering high dynamic range image, Proc. SPIE Image Sensor 3965 (2001) 392–401.
[29] S. Dippel, M. Stahl, R. Wiemker, T. Blaffert, Multi-scale contrast enhancement for radiographies: Laplacian pyramid versus fast wavelet transform, IEEE Trans. Med. Imaging 21 (4) (2002) 343–353.
[30] B. Wandell, Foundations of vision, Sinauer Associates, 1995.
[31] A. Lain, J. Fan, S. Sculer, A Framework for Contrast Enhancement by Dyadic Wavelet Analysis: Digital Mammography, Elsevier, Amsterdam, 1994.
[32] T.J. Brown, An adaptive strategy for wavelet based image enhancement, Proc. IMVIP 2000 5 (1998) 67–81.
[33] X.A. Zong, F. Laine, E.A. Geiser, D.C. Wilson, Denoising and contrast enhancement via wavelet shrinkage and non-linear adaptive gain, Wavelet Applications 3: Proc. SPIE 2763 (1996) 566–574.
[34] M.D. Levine, Vision in Man and Machine, McGraw-Hill, New York, 1985.
[35] J.A. Ferwerda, S.N. Pattanaik, P. Shirley, A model of visual adaptation for realistic image synthesis, Proc. SIGGRAPH (1996) 245–258.
[36] S.S. Stenvens, To honor Fechner and repeal his law, Science 13 (1961) 80–86.
[37] R.G. Hunt, The production of color. Fountain Press, fifth ed., Kingston upon Thames, England, 1996.

[38] S.N. Pattanaik, A multiscale model of adaptation and spatial vision for realistic image display, Proc. SIGGRAPH (1998) 287–298.

[39] D. Laming, J.J. Kulikowski, V. Walsh, I.J. Murray (Eds.) Contrast sensitivity in limits of vision, v.5, Vision and Visual Dysfunction. CRC Press, Boca Raton, FL, 1991 pp. 35–43.

[40] G.W. Larson, H. Rushmerier, C. Piatko, A visibility matching tone reproduction operator for high dynamic range scenes, IEEE Trans. Visual. Comput. Graph. 3 (4) (1997) 291–306.

[41] E. Peli, Contrast in complex images, J. Optical Soc. Am. A. 7 (1990) 2032–2040.

[42] G.D. Finlayson, S.D. Hordley, P.M. HubeL, Color by correlation: a simple, unifying framework for color constancy, IEEE Trans. Pattern Anal. Mach. Intell. 23 (11) (2001) 1209–1221.

[43] F. Ebner, M.D. Fairchild. Development and testing of a color space (IPT) with improved hue uniformity, IS&T/SID 6th Color Imaging Conference, Scottsdale (1998) 8–13.

[44] S. Daly, The visible differences predictor: an algorithm for the assessment of image fidelity, in: A. Watson (Ed.), Digital Images and Human Vision, MIT, Cambridge, 1993.

[45] J. Lubin, The use of psychophysical data and models in the analysis of display system performance, in: A. Watson (Ed.), Digital Images and Human Vision, MIT, Cambridge, 1993.

[46] M.J. Shensa, Discrete wavelet transforms: wedding the à trous and Mallat algorithms, IEEE Trans. Signal Process. 40 (1992) 2464–2482.

[47] <http://www.media.hut.fi/~color/sample_images.html/>.

[48] <http://www.cs.utah.edu/~reinhard/cdrom//>.